

pubs.acs.org/accounts Article

Metal—Ligand Interactions and Their Roles in Controlling Nanoparticle Formation and Functions

Published as part of the Accounts of Chemical Research special issue "Ligand and Surface Chemistry of Nanoparticles".

Huanqin Guan, Cooro Harris, and Shouheng Sun*



Cite This: Acc. Chem. Res. 2023, 56, 1591-1601

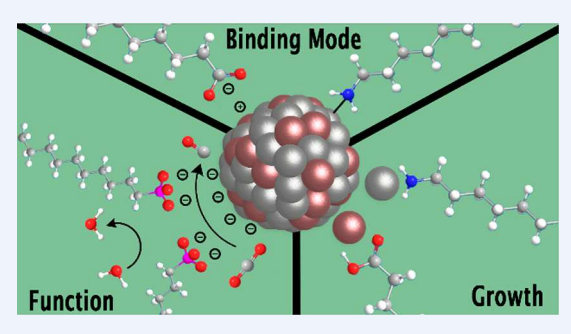


ACCESS I

Metrics & More

Article Recommendations

CONSPECTUS: Functional nanoparticles (NPs) have been studied extensively in the past decades for their unique nanoscale properties and their promising applications in advanced nanosciences and nanotechnologies. One critical component of studying these NPs is to prepare monodisperse NPs so that their physical and chemical properties can be tuned and optimized. Solution phase reactions have provided the most reliable processes for fabricating such monodisperse NPs in which metalligand interactions play essential roles in the synthetic controls. These interactions are also key to stabilizing the preformed NPs for them to show the desired electronic, magnetic, photonic, and catalytic properties. In this Account, we summarize some representative organic bipolar ligands that



have recently been explored to control NP formation and NP functions. These include aliphatic acids, alkylphosphonic acids, alkylamines, alkylphosphines, and alkylthiols. This ligand group covers metal-ligand interactions via covalent, coordination, and electrostatic bonds that are most commonly employed to control NP sizes, compositions, shapes, and properties. The metal-ligand bonding effects on NP nucleation rate and growth can now be more thoroughly investigated by in situ spectroscopic and theoretical studies. In general, to obtain the desired NP size and monodispersity requires rational control of the metal/ligand ratios, concentrations, and reaction temperatures in the synthetic solutions. In addition, for multicomponent NPs, the binding strength of ligands to various metal surfaces needs to be considered in order to prepare these NPs with predesigned compositions. The selective ligand binding onto certain facets of NPs is also key to anisotropic growth of NPs, as demonstrated in the synthesis of onedimensional nanorods and nanowires. The effects of metal-ligand interactions on NP functions are discussed in two aspects, electrochemical catalysis for CO₂ reduction and electronic transport across NP assemblies. We first highlight recent advances in using surface ligands to promote the electrochemical reduction of CO₂. Several mechanisms are discussed, including the modification of the catalyst surface environment, electron transfer through the metal-organic interface, and stabilization of the CO₂ reduction intermediates, all of which facilitate selective CO2 reduction. These strategies lead to better understanding of molecular level control of catalysis for further catalyst optimization. Metal-ligand interaction in magnetic NPs can also be used to control tunneling magnetoresistance properties across NPs in NP assemblies by tuning NP interparticle spacing and surface spin polarization. In all, metal-ligand interactions have yielded particularly promising directions for tuning CO₂ reduction selectivity and for optimizing nanoelectronics, and the concepts can certainly be extended to rationalize NP engineering at atomic/molecular precision for the fabrication of sensitive functional devices that will be critical for many nanotechnological applications.

KEY REFERENCES

• Shen, M.; Yu, C.; Guan, H.; Dong, X.; Harris, C.; Xiao, Z.; Yin, Z.; Muzzio, M.; Lin, H.; Robinson, J. R.; Colvin, V. L.; Sun, S. Nanoparticle-Catalyzed Green Chemistry Synthesis of Polybenzoxazole. J. Am. Chem. Soc. 2021, 143, 2115–2122. The paper reported the synthesis of AuPd alloy nanoparticles with oleylamine as a protection ligand and the removal of oleylamine to catalyze tandem reactions in a green chemistry reaction condition.

 Guan, H.; Shen, M.; Harris, C.; Lin, H.; Wei, K.; Morales, M.; Bronowich, N.; Sun, S. Cu₂O nanoparticlecatalyzed tandem reactions for the synthesis of robust

Received: March 10, 2023 Published: May 19, 2023





polybenzoxazole. Nanoscale **2022**, 14, 6162-6170. The phosphonic acid ligand was used to control the synthesis of monodisperse Cu nanoparticles, their oxidation to Cu₂O nanoparticles, and enhanced catalysis for tandem reactions leading to green chemistry synthesis of polybenzoxazole.

- Fu, J.; Zhu, W.; Chen, Y.; Yin, Z.; Li, Y.; Liu, J.; Zhang, H.; Zhu, J.-J.; Sun, S. Bipyridine-Assisted Assembly of Au Nanoparticles on Cu Nanowires to Enhance the Electrochemical Reduction of CO₂. Angew. Chem. Int. Ed. 2019, 58, 14100–14103.³ The ligand bipyridine served as a linker between Au nanoparticles and Cu nanowires to enable tandem electrocatalysis in CO₂ reduction.
- Lv, Z.-P.; Luan, Z.-Z.; Wang, H.-Y.; Liu, S.; Li, C.-H.; Wu, D.; Zuo, J.-L.; Sun, S. Tuning Electron-Conduction and Spin Transport in Magnetic Iron Oxide Nanoparticle Assemblies via Tetrathiafulvalene-Fused Ligands. ACS Nano 2015, 9, 12205–12213. The tetrathiafulvalene-COOH ligand was used to stabilize Fe₃O₄ nanoparticles and to control magneto-electronic transport in the Fe₃O₄ nanoparticle array.

1. IMPORTANCE OF LIGAND BINDING IN NANOPARTICLE CHEMISTRY

Over the past decades, nanosized (1–100 nm) particles, or more commonly nanoparticles (NPs), have received evergrowing interest due to their unique properties that have emerged in this length scale, which are not seen from either their bulk or molecular counterparts. The distinctive optical, electronic, magnetic, and surface properties demonstrated by these NPs have shown great application potentials in electronics, photonics, magnetics, catalysis, and biomedicine. As these properties are dictated by NP sizes, shapes, compositions, and structures, it has become critically important to prepare NPs with controllable functions, manageable stability, and tunable performance for the targeted applications.

Both inorganic and organic materials can be made into NPs. In this Account, we focus on NPs containing inorganic materials, especially metals and metal oxides, with distinctive physical and chemical functions. Each of these NPs is composed of a functional inorganic core and an organic ligand shell. This shell is formed by an array of organic ligands (also commonly denoted as surfactants, stabilizing agents, or capping agents) and plays important roles in controlling NP growth, stabilization, and postsynthetic modification for various applications. These ligands often contain polar head groups, which are used to bind to metals on the NP surface, and nonpolar tails, which are packed on the NP surface, stabilizing NPs against aggregation and controlling NP functionality. The binding chemistry between the polar heads and NP surface atoms is similar to metal-ligand interactions in coordination chemistry and is critical to NP formation and stabilization. A variety of head groups have been explored to saturate the dangling bonds of the exposed atoms on the NP surfaces for NP passivation and stabilization. 16 The direct metal-ligand binding can be used to control the growth of NPs into different sizes and geometric shapes, while the steric bulkiness of the hydrocarbon chains can influence the permeability of the reactant to the surface of NPs, which determines the directional growth rate of the NPs. Longer or branched ligands can form a densely packed coating around

each NP and often result in the formation of smaller NPs. Furthermore, the postsynthetic modification of the existing ligands or replacement of the original ligands with new ones have been essential for extending the versatility of NPs to better suit the end applications. For example, to prepare NPs for biomedical applications, the NPs need to be biocompatible, traceable, and target-specific. This is usually achieved by modifying the NP surfaces with a group of biocompatible molecules, such as organic dyes, polymers, peptides, DNAs, or antibodies. The surface ligands can also help to promote NP's catalytic activity, selectivity, and durability via their electronic/steric effects.

In this Account, we summarize some representative metalligand interactions and their roles in controlling NP formation and functions. We first introduce a series of common ligands and their typical binding modes on NP surfaces. The strength of these metal-ligand interactions can be tuned by changing the coordination environment. We will then review the ligand effects on NP growth and stabilization in solution phase synthesis conditions. Representative examples on how to use ligands and their combinations to control NP sizes, shapes, and compositions are highlighted. Lastly, we discuss how to use ligand coating to enhance NP catalytic activity and selectivity, as well as to control interparticle spacing in NP arrays to improve electron transport across the arrays. NP modification with ligands for biomedical applications is an extremely important topic in the nanomedicine field and has been extensively reviewed elsewhere. 19-22 Readers who are interested in learning these biomedical aspects of NPs are suggested to check these or other reviews.

2. COMMON LIGANDS AND THEIR BINDING MODES

For a ligand to be applicable to bind to NPs, it must first be chemically stable in NP synthetic conditions with only the polar group interacting with the surface atoms of the NPs and the tail group providing a layer of coating around each NP. This makes the bipolar molecules with a functional headgroup and a stable hydrocarbon tail a universal ligand choice in organic phase reactions for the synthesis of monodisperse NPs. The capability of a ligand to influence the surface energy and growth of a NP is strongly dependent on the available binding modes of the ligand to the metal atoms, and if this binding event can reach equilibrium in the reaction condition then too strong a binding may render the metal precursor too stable to nucleate, while too weak a binding may not provide enough protection to the formed NPs against the uncontrollable growth and aggregation from the reaction medium. Various ligands used for the NP synthesis have been reported. 6,15,16,23-25 Here we focus on some common organic ligands that have been extensively explored in recent years for the synthesis of monodisperse NPs in organic phase reactions with the desired function controls. These include aliphatic acids (RCOOH), alkylphosphonic acids (RPO₃H), alkylamines (RNH₂), trialkylphosphines (R₃P), and alkylthiols (RSH), each of which contains a functional group that can bind to different metals with unique binding modes and binding affinities. Figure 1 illustrates different binding modes of these functional groups on a metal (M) surface via covalent (RCOO-M, RPO₃-M, and RS-M), coordination (RNH₂ \rightarrow M, $R_3P \rightarrow M$), and electrostatic (R_4N^+) bonding modes.^{5,26} In general, the binding affinity is increased in the order of electrostatic, coordination, covalent interactions, and can be better explained by the "hard and soft (Lewis) acids and bases"

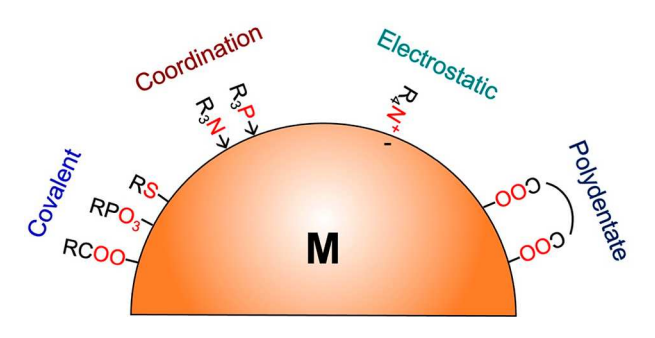


Figure 1. Binding modalities of common ligand functional groups to the surface of a generic metal NP.

concept.²⁷⁻²⁹ For example, the "harder" O-based ligands are better applied to bind the first-row transition metal (M) via RCOO-M, while the "softer" RS-based or R₃P-based ligands are more suitable to bind to late transition/noble metals via RS-M or R₃P-M. RNH₂ has a borderline Lewis basicity when compared to "O"- and "S"-based binding groups and can be applied to bind to either first-row or late transition metals in the synthesis. Exactly what kind of ligand to choose to modify NPs is dependent on the need for next-step studies. For example, Au NPs are commonly prepared in the presence of a thiol ligand, where the strong Au-S covalent bond offers a robust protection of Au NPs for long-term stability. However, when studying the catalytic properties of these Au NPs, this strong Au-S bonding can deactivate Au NPs, making them catalytically inactive.³⁰ The strong Au-S bonding also makes it difficult to remove thiol coating without affecting NP properties. A synthetic solution to this problem is to use RNH₂ as a ligand to control the Au NP growth and stabilization.31 Au NPs modified with RNH2 can be easily activated for catalysis studies even for the Au NPs that are sensitive for further treatment.³² The RNH₂-M binding affinity can also be tuned easily in the reaction medium. A good example of this tunable binding mode change is seen in the RNH2-Pt NPs under basic and acidic conditions. The spectroscopic study on the binding modes showed that the strong coordination bonding from RNH2 to Pt shifted to a

much weaker electrostatic interaction at lower pH due to the protonation of RNH₂. ³³ Such a pH-induced bonding mode change between RNH₂ and noble metals has been commonly used as a method for amine-based ligand removal from noble metal NPs. ¹ Therefore, it has become a routine strategy to remove amine coating on the noble metal NP surface by a simple acid washing process. Ligand binding affinity can be further enhanced by controlling the binding mode from monodentate to polydentate (Figure 1). The polydentate ligand binding is often applied to where the ligand is required to bind NPs tightly so that the ligand shell is not disrupted in next-step applications, as seen in stabilizing NPs for biomedical applications.

3. LIGAND EFFECTS ON CONTROLLING NANOPARTICLE FORMATION

In the organic phase synthesis of NPs, a ligand plays an essential role in controlling NP formation and growth, as outlined in Figure 2a. First, the common metal precursor is generally a salt, which is not easily dissolved in a high-boiling hydrocarbon solvent that is used to facilitate fast nucleation and growth of NPs unless an organic ligand is present. Second, the ligand binding helps to control at what stage the metal atoms can form stable nuclei, a process that is thermodynamically unfavored and requires energy input (often via increasing the reaction temperature) to accomplish. Third, once the nuclei are formed, the following growth process is thermodynamically favored and spontaneous as long as there are enough metal precursors present in the reaction system. Therefore, the ligand coating at this growth stage is also essential for capturing NPs at their proper size range and stabilizing them in the solution state against uncontrolled growth into aggregates. Fourth, the hydrocarbon nature of the ligand tails renders the NPs hydrophobic, which makes it possible to separate these NPs from the reaction mixture by adding a polar solvent. Finally, the ligand captured NPs can be easily purified and dispersed in a fresh solvent for further use. Recently, more detailed understanding of ligand effects on NP nucleation and growth is demonstrated by using in situ small-

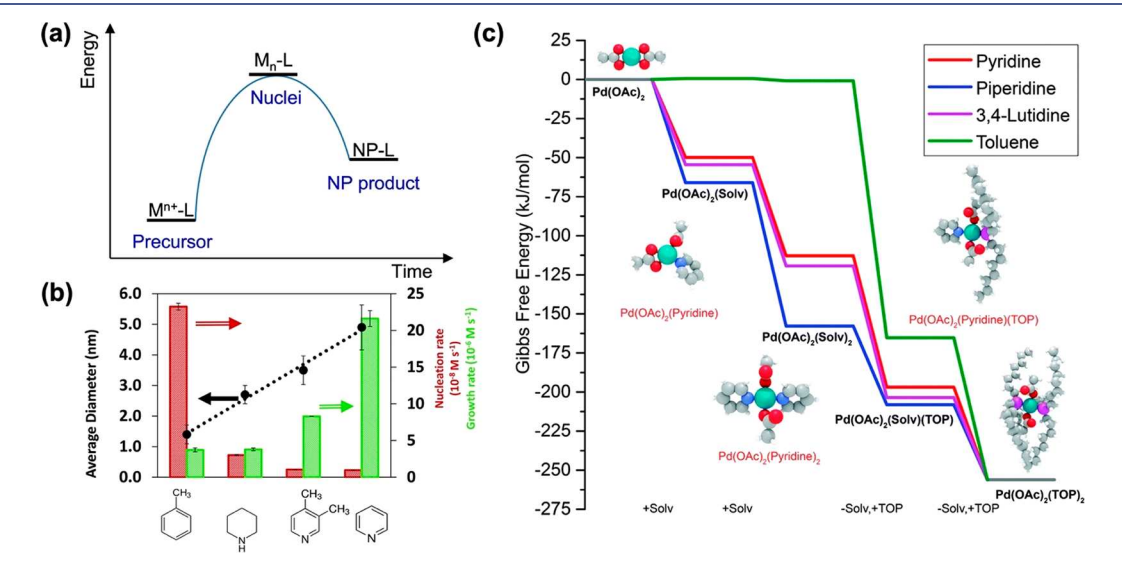


Figure 2. (a) Schematic energy diagram of M-L energy level change in NP synthesis. (b) Correlation between nucleation/growth and average NP size measured in the different solvents. The dotted lines indicate the observed size trend. (c) Gibbs free energy of different Pd-L complexes: Pd, teal; N, light blue; H, white; O, red; P, magenta; and C, gray.³⁴

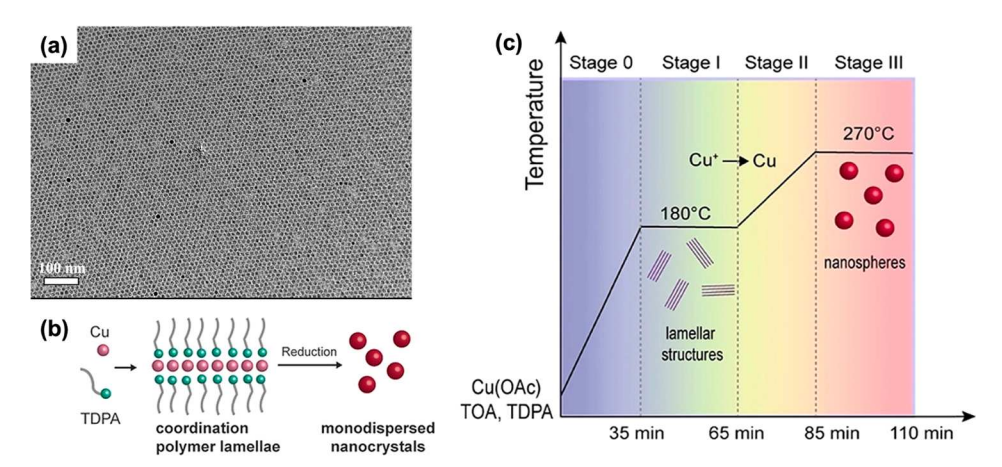


Figure 3. (a) TEM image of the monodisperse Cu NPs (7 nm) showing a hexagonal packing pattern.² (b) Sketch of the conversion of the TDPA-Cu coordination polymer lamellae into monodisperse Cu NPs. (c) Synthesis scheme for the formation of Cu NPs involving the decomposition of lamellar polymer.³⁵

angle X-ray scattering during the synthesis of Pd NPs in the presence of trioctylphosphine.³⁴ The study shows a clear correlation between nucleation/growth rates and the thermodynamics of metal-ligand/solvent binding (Figure 2b): when the nucleation rate decreases, the growth rate increases in the order of toluene, piperidine, 3,4-lutidine, and pyridine. This indicates that when the solvent has no coordination power, such as in toluene, the atomic state Pd is much better stabilized by the phosphine coating, making it difficult to nucleate/grow. When the ligand binding power increases from piperidine, 3,4lutidine, and pyridine, the phosphine ligand binding is interrupted due to the N-binding competition, leading to easy nucleation and growth of NPs. This is further supported by density functional theory (DFT) calculated Gibbs free energies of the solvent-dependent dominant Pd-complex and the solvent-NP binding energy (Figure 2c). It shows that the stronger the ligand (solvent) binding, the slower the nucleation rate due to the metal precursor being better stabilized, making it more difficult to reduce the metal precursor. On the other hand, strong ligand binding power also slows the rate of NP growth due to the lack of active sites on the preformed NP surface.

In the NP formation process, the relative molar ratio of metal precursors to ligand, as well as their concentrations, in the reaction system can also have dramatic effects on the NP size and stability. This has been broadly demonstrated in solution phase synthesis of NPs, including the recent synthesis of monodisperse Cu NPs by reduction of the copper acetate (CuOAc) precursor in the presence of the tetradecylphosphonic acid (TDPA) ligand. 2,35 By controlling the relative metal-to-ligand molar ratio to 1:0.5, 1:0.75, and 1:1, respectively, monodisperse 7, 9, and 12 nm Cu NPs were made, as shown in Figure 3a. 2 16 nm Cu NPs were prepared by increasing the concentration of both CuOAc and TDPA from 0.1 mol/L to 0.2 mol/L while using the same 1:0.5 ratio as in the 7 nm Cu NP synthesis. The ligand effect can be observed directly through an in situ X-ray characterization study on the synthesis of Cu NPs.35 In the similar synthetic condition, the TDPA ligand was found to form a lamellar coordination polymer with Cu⁺ ions at 180 °C, which was identified as a nucleation hotspot for the size monodispersity (Figure 3b). Careful in situ analysis with small-angle X-ray scattering and X-ray diffraction during the Cu NP synthesis

clearly illuminates the Cu metal transition from $\text{Cu}^+ \to \text{Cu}^0$ and the formation and decomposition of the TDPA-Cu⁺ lamellar structures as temperature increases (Figure 3c). Using this information, Cu NPs with size range of 3–26 nm were synthesized.

Metallic alloy or other multicomponent NPs can be synthesized by controlling M-L interactions as long as each component has similar M-L binding properties, as seen in the oleylamine-mediated synthesis of various alloy NPs. 36,37 However, when M-L binding chemistry differs greatly from each other, to control alloy NP composition requires the use of different ligands to ensure nucleation and growth of NPs with composition controls. The synthesis of FePt NPs is a good example to highlight the importance of different ligand effects on the controllable formation of multicomponent NPs. 38,39 FePt NPs were synthesized by thermal decomposition of $Fe(CO)_5$ and reduction of $Pt(acac)_2$ (acac, acetylacetonate). These two precursors have very different reaction chemistry as Fe(CO)₅ is easily decomposed to form magnetic Fe NPs, while Pt(acac)₂ is easily reduced. When only an oleylamine ligand was used in the synthesis, the synthesis tended to yield Pt-rich FePt NPs. To obtain Fe-rich FePt NPs, oleic acid must also be present. More oleic acid led to Fe-rich FePt NPs, while more oleylamine resulted in Pt-rich FePt NPs. To prepare FePt NPs with near 1/1 Fe/Pt ratio for magnetic property control, oleic acid and oleylamine should be present in equal molar ratio. Under this synthetic condition, both RCOO-Fe and RNH2-Pt need to be present to control Fe/Pt nucleation/growth and to stabilize the FePt NPs after the synthesis (Figure 4a,b). This combination of ligand effects has become a reliable approach to prepare various NPs with surfaces having multicompositions or multioxidation states. 40

As the M-L binding affinity depends not only on orbital energy but also on orbital symmetry, 41 this binding can be anisotropic on a NP surface with different crystal facet exposures, which infers that a NP can grow into an anisotropic shape if the synthetic condition and M-L binding strength are carefully controlled. An under-stabilized facet is prone to grow at a faster rate than the stabilized one, which leads to anisotropic growth of NPs, as seen in the growth of CdSe nanorods in the presence of hexylphosphonic acid (HPA, $C_6H_{13}P(O)(OH)_2$) and the synthesis of Cu_2S nanodiscs in the presence of alkylthiol ligand. 42 CdSe nanorods are formed due

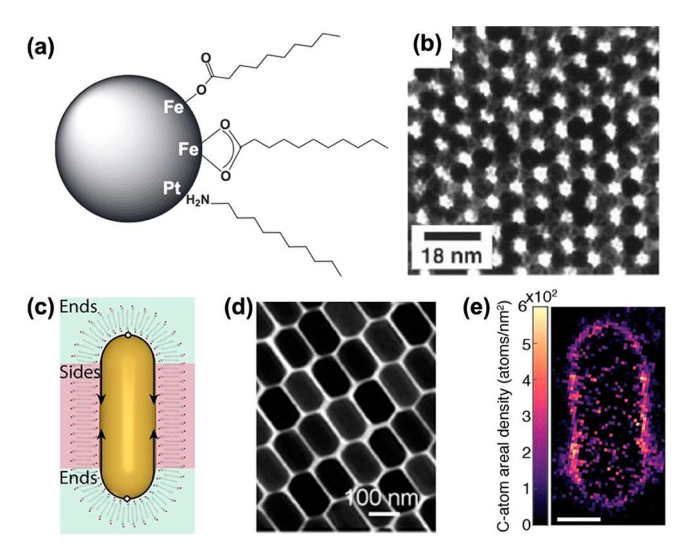


Figure 4. (a) Schematic surface binding of different ligands for composition-controlled synthesis and stabilization of FePt NPs. (b) TEM image of FePt NPs stabilized by RCOO-Fe and RNH₂-Pt. 38 (c) Nanorod surrounded by an elongated micellar coating. (d) TEM image of the Au nanorods synthesized using a CTAB-NaOL mixture in the growth solution. (e) EELS carbon compositional map of a CTAB-coated Au nanorod. Scale bar = 10 nm. 44

to the selective HPA binding to the {100} and {110} facets of the seeding NPs, which promotes the growth of NPs preferably along the [001] direction, yielding a rod-shape. For Cu₂S NPs, alkylthiol can strongly bind to the {001} faces, suppressing the growth along this direction, and resulting in the formation of disc-shaped Cu₂S NPs. The anisotropic shape of NPs can also be controlled by seed-mediated growth of polyhedral NPs in a nonspherical reverse micelle structure formed by ligand assembly in the reaction solution. In this micellar structure, NP growth can be further facilitated along the micellar structure as long as there is enough NP-precursor present in the reaction solution. The formation of Au nanorods is an excellent example to demonstrate this concept.⁴³ These Au nanorods are formed via the seed-mediated growth of Au NPs in the presence of the structure-directing ligand, cetyltrimethylammonium bromide (CTAB). CTAB preferentially binds to the sides of the rod-shaped NPs, stabilizing the sides more efficiently, and allowing the fast growth at both ends where ligands are less densely packed, leading to the formation of Au nanorods (Figure 4c). The quality of the nanorod product can be further improved by introducing a coligand to the CTAB system. For example, by mixing CTAB with sodium oleate (RCOONa, NaOL), more uniform Au nanorods are prepared (Figure 4d). This anisotropic distribution of the ligands around each Au nanorod was recently visualized and quantified by electron energy loss spectroscopy (EELS) (Figure 4e).⁴⁴ The study proves that the distribution of CTAB on Au nanorods is anisotropic, and the ligand at the ends has a 30% decrease in density compared with that around the sides. Oleylamine is also a popular ligand to use to form reverse micelle structures in which nanowires can grow. This have been demonstrated in the synthesis of ultrathin Au and MPt nanowires. 32,45 For example, in preparing FePt nanowires via thermal decomposition of Fe(CO)₅ and reduction of Pt(acac)₂, the nanowire length control was realized by tuning the volume ratio between oleylamine (ligand) and 1-octadecene (solvent): FePt nanowires longer than 200 nm were made when only oleylamine

was used as both surfactant and solvent, while a ligand/solvent ratio of 3:1 gave 100 nm FePt nanowires and a 1:1 volume ratio led to 20 nm FePt nanowires. When a larger volume of solvent was used, for example, ligand/solvent ratio = 1/3, the cylinder-shaped reverse micelle was disrupted by the presence of a large amount of solvent, and as a result, 3 nm spherical FePt NPs were obtained. DFT calculations have been used to understand the origin of specific shape formation by comparing the adsorption energy between the ligands and low index metal NP surfaces. Previous studies found that the formation of the AgPt alloy nanowires was mostly driven by the interplay between the binding energy of ligands on the alloy surface and the diffusion of atoms at the interface upon their collision with primary NPs. 46

4. LIGAND EFFECTS ON CONTROLLING NANOPARTICLE FUNCTIONS

4.1. Ligand Effect on Nanoparticle Catalysis

Understanding M-L binding chemistry has become an important topic in NP catalysis, especially electrocatalysis for energy conversion reactions, such as the electrochemical CO2 reduction reaction (CO₂RR).⁴⁷ Traditionally, the ligand molecules binding on the surface are believed to block the surface sites and thus lower the catalytic activity. 48 However, in recent decades, there have been numerous studies exploring the beneficial role of ligands in defining the catalytic environment and enhancing the electrocatalytic performance by various mechanisms.⁴⁹ In fact, the presence of ligands on metal surfaces introduces additional complexities to this metal-organic system, including the modification of the catalyst surface environment, electron transfer through the metal-organic interface, and stabilization of the CO2 reduction intermediates.⁵⁰ All these effects due to metalligand interaction could contribute to better activity, selectivity, and durability for the CO₂ electrocatalysis.

The common organic ligand used for metal, especially noble metal, NP surface modification is RSH due to its great binding affinity to noble metals. There have been numerous studies in modifying catalyst surfaces with thiols to improve the CO₂RR selectivity. Thiol-terminated imidazolium with different alkyl chain length was used to modify the Au electrode to improve the CO_2 reduction selectivity for the formation of ethylene glycol. In this study, the Au catalysis exhibited a ligand length-dependent property with 1-(-2-mercaptoethyl)-3-methylimidazolium bromide (IL-2)-modified Au showing the highest Faradaic efficiency (FE) of 87% toward ethylene glycol. Such enhancement in selectivity to ethylene glycol was attributed to more efficient coupling of imidazolium aldehyde intermediates in the reaction condition. In the presence of a longer ligand chain on the Au surface, the interaction between imidazolium and Au gets weaker, limiting the charge transfer for the formation of imidazolium aldehyde intermediates. Despite the evident impact of these thiols on metal catalysis, the long-standing catalyst durability issue in the CO₂RR remains. Efforts have been made to improve the stability of NP catalysts in CO2 reduction reactions through the introduction of N-heterocyclic carbene (NHC) ligands. 52,53 NHCs bind with metals by utilizing the lone electron pair on carbon, creating a strong M-C σ bond. ⁵⁴ This bond has been applied to modify the surfaces of different metals, enhancing their stability. Stability. Furthermore, the σ -donation from NHCs increases the charge density on metal surfaces, resulting in better metal

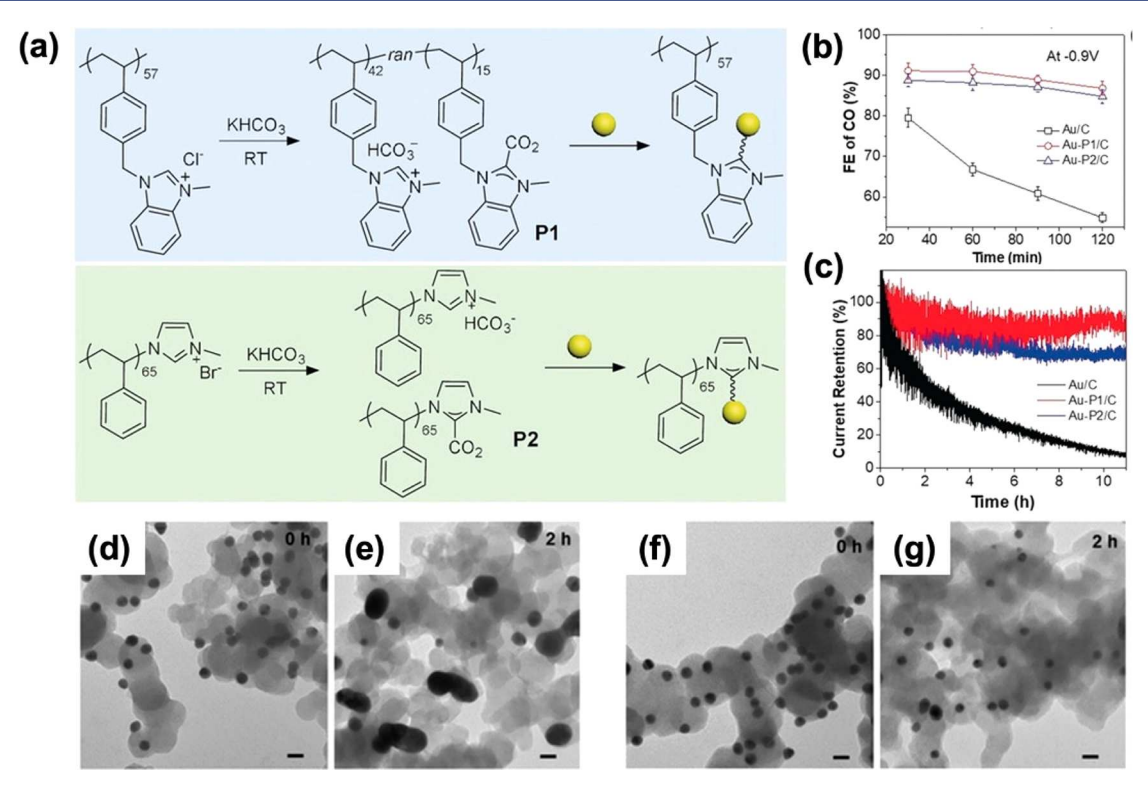


Figure 5. (a) Schematic illustration of synthesis of P1, P2, and surface modification of NPs (yellow). (b) CO FE at -0.9 V for different electrolysis times. (c) Long-term stability plotted as current retention versus time at -0.9 V for 11 h. TEM images of Au/C (d, e) and Au-P1/C (f, g) before and after CO₂ reduction at -0.9 V for 2 h. All scale bars are 20 nm. 52

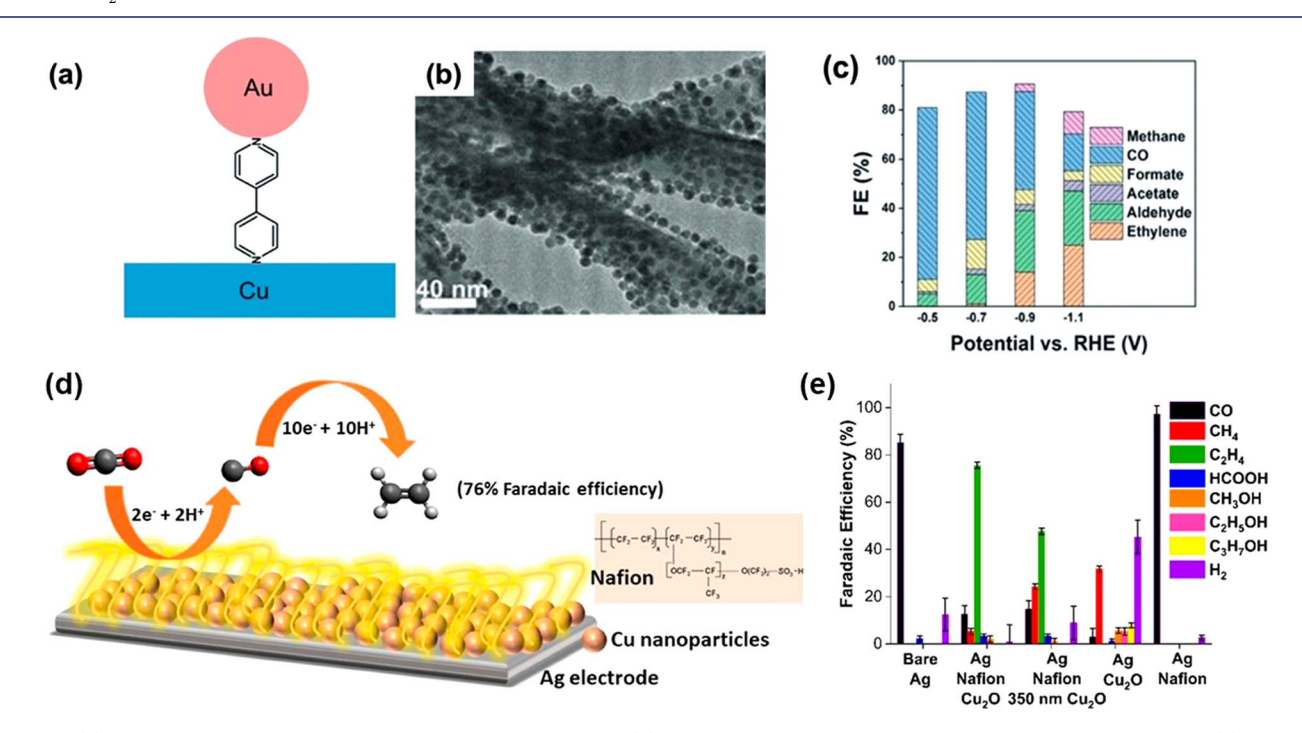


Figure 6. (a) Schematic illustration of Au-bipy-Cu composite catalyst. (b) TEM image of Au-bipy-Cu with Au/Cu atomic ratio of 1:1. (c) Total FE of the Au-bipy-Cu catalyzed CO_2RR at different potentials.³ (d) Schematic illustration of Nafion coupled Cu NPs on Ag electrode for tandem CO_2RR to C_2H_4 . (e) FE for CO (black), CH_4 (red), C_2H_4 (green), HCOOH (blue), CH_3OH (orange), C_2H_5OH (pink), C_3H_7OH (yellow), and CO_2RR after 1 h of CO_2 reduction at CO_2RR at different potentials.³ (d) Schematic illustration of Nafion coupled Cu NPs on Ag electrode for tandem CO_2RR to CO_2H_4 . (e) FE for CO (black), CO_2H_4 (green), HCOOH (blue), CO_3H_4 (green), HCOOH (blue), CO_3H_4 (purple) after 1 h of CO_2 reduction at CO_2RR at different potentials.³ (d) Schematic illustration of Nafion coupled Cu NPs on Ag electrode for tandem CO_2RR to CO_2H_4 . (e) FE for CO_2RR at different potentials.³ (d) Schematic illustration of Nafion coupled Cu NPs on Ag electrode for tandem CO_2RR to CO_2RR at different potentials.³ (d) Schematic illustration of Nafion coupled Cu NPs on Ag electrode for tandem CO_2RR to CO_2RR at different potentials.³ (d) Schematic illustration of Nafion coupled Cu NPs on Ag electrode for tandem CO_2RR to CO_2RR (purple) after 1 h of CO_2RR (purple) after 1 h of CO

binding with CO₂ as an electrophile. In one study, two NHC polymers (P1 and P2) were grafted onto the 14 nm Au NPs for CO₂RR (Figure 5a).⁵² Both Au–P1/C and Au–P2/C showed higher activity and selectivity than the Au/C due to the

formation of a hydrophobic layer to suppress hydrogen evolution reaction (HER) (Figure 5b). The NHC-modified Au nanocatalysts showed an activity retention of 86% at -0.9 V after CO₂ electrolysis for 11 h, which is much higher than

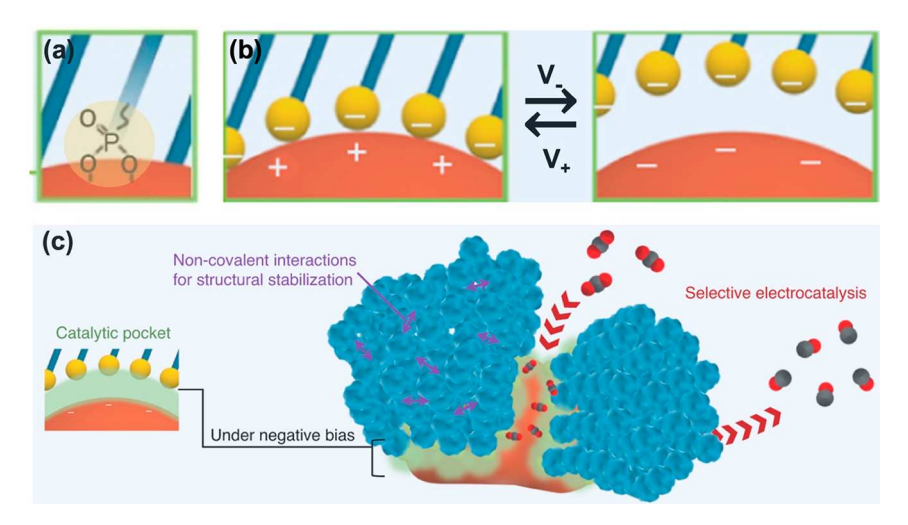


Figure 7. (a) Schematic of phosphonate binding mode. (b) Schematic of the NP/ligand interlayer with ligands desorbing and adsorbing reversibly under biased conditions. (c) Schematic illustration of the NP/ligand interlayer catalytic pocket for selective CO₂ reduction to CO (C, black; O, red). ST

that for the unmodified Au of 10% (Figure 5c). Compared with other thiol and amine ligands, the NHC can effectively stabilize NPs against aggregation under reductive potentials (Figure 5d-g).

The ligands can also bridge two different catalysts so that their catalysis can be coupled to promote tandem catalysis. In a recent demonstration, Au NPs were attached to Cu nanowires through a 4,4'-bipyridine (bipy) linker to form the new composite catalyst Au-bipy-Cu (Figure 6a).³ Au is known to be selective in catalyzing CO₂RR to CO, while Cu is more active to catalyze the CO reduction to hydrocarbon products. Because of the close proximity between Au and Cu, the newly formed CO around Au can be transferred to Cu sites where it is reduced to multicarbon products. This process is further enhanced by the presence of bipy between Au and Cu that, as a Lewis base center, can help to stabilize the CO₂^{-*} intermediates and enrich protons near the catalyst surface, facilitating the CO₂RR. The catalysis of the Au-bipy-Cu catalyst can also be tuned by the Au/Cu atomic ratios. The Aubipy-Cu catalyst with the Au/Cu atomic ratio of 50% (Figure 6b) catalyzed the CO₂RR to carbon products with a total FE reaching 90% at -0.9 V versus RHE (Figure 6c). Similarly, Nafion was used as a polymeric linker to couple Cu NPs with the Ag electrode to enhance the tandem electroreduction of CO₂ (Figure 6d).⁵⁶ As a hydrophilic polymer, Nafion is believed to facilitate mass transport of the reactive CO intermediates and protons, enabling the stepwise reaction pathway and enhancing the CO2RR selectivity. As such, CO2 is first reduced to CO on Ag, and then CO, along with protons, is regulated by Nafion to Cu NPs and subsequently reduced to C₂H₄. Due to the synergistic effect among Ag-Nafion-Cu, the composite catalyst showed a high selectivity toward C2H4 (76% FE) (Figure 6e).

Recently, a new strategy was developed to improve CO₂RR in a pseudocapacitive NP/ligand interlayer.⁵⁷ In this study, the interlayer structure was first built by binding tetradecylphosphonate (CH₃(CH₂)₁₃PO₃²⁻) on the Ag NP surface via a bidentate bonding mode (Figure 7a). The ligand layer is tightly associated and can adsorb/desorb reversibly from each Ag NP under biased conditions (Figure 7b). In the reductive CO₂RR condition, the adsorbed phosphonate ligands dissociated from the Ag NP surface, creating a pseudocapacitive pocket without

disrupting the overall ligand assembly structure, allowing K⁺ to diffuse in to balance the charge. The hydrophobic coating around the pocket structure facilitates the diffusion of CO_2 , while inhibiting the diffusion of water/protons, into the interlayer structure, favoring CO_2 conversion over the HER (Figure 7c). As a result, the CO_2 to CO conversion reached 97%. In a gas diffusion electrode in 1 M KHCO₃, the structure catalyzed CO_2RR with 98.1% CO selectivity at 400 mA/cm² and 2921 A/g_{Ag}. This idea can be extended to couple oleate $(CH_3(CH_2)_7CH = CH(CH_2)_7COO^-)$ and other NPs, such as Au and Pd NPs, creating similar interlayer structures to enhance NP-catalysis for the CO_2 reduction to CO.

4.2. Ligand Effects on Electron Transport Across Assembled Nanoparticles

Ligand effects on NP assemblies have been extensively studied, and such studies continue to be a hot topic in the nanomaterials research field. Ligand coating on the NP surface provides an effective way to control interparticle spacing in a NP array, facilitating the study of the correlated properties arising from the interactive NP network. Here we focus on one example on understanding magneto-transport of electrons across the NP arrays for potential nanoelectronic applications. 5,60,61 In the past, magnetoresistance (MR) effect of the layered nanostructures has led to the development of highly sensitive magnetic devices, including tunneling magnetoresistance (TMR) devices, for sensing applications.8 Magnetic NPs prepared from solution phase synthesis with tunable surface ligands and magnetic NP arrays formed from their self-assemblies are ideal for studying TMR. Among various NPs that have been studied for TMR, half-metallic magnetic Fe₃O₄ NPs are especially promising as a practical material because of its strong ferrimagnetism, high spin polarization at the Fermi level, and high Curie temperature.⁶² Despite their potential as demonstrated in studies of spindependent transport, Fe₃O₄ NPs face a significant drawback that they are prone to oxidation under ambient conditions, resulting in a loss of conductivity and limiting their practical use. To stabilize the Fe₃O₄ NPs and regulate their assembly properties, tetrathiafulvalene carboxylic acid (TTF-COOH) was applied to modify the NP surface. 4 TTF units have a rigid planar structure and are excellent electron donors, which help

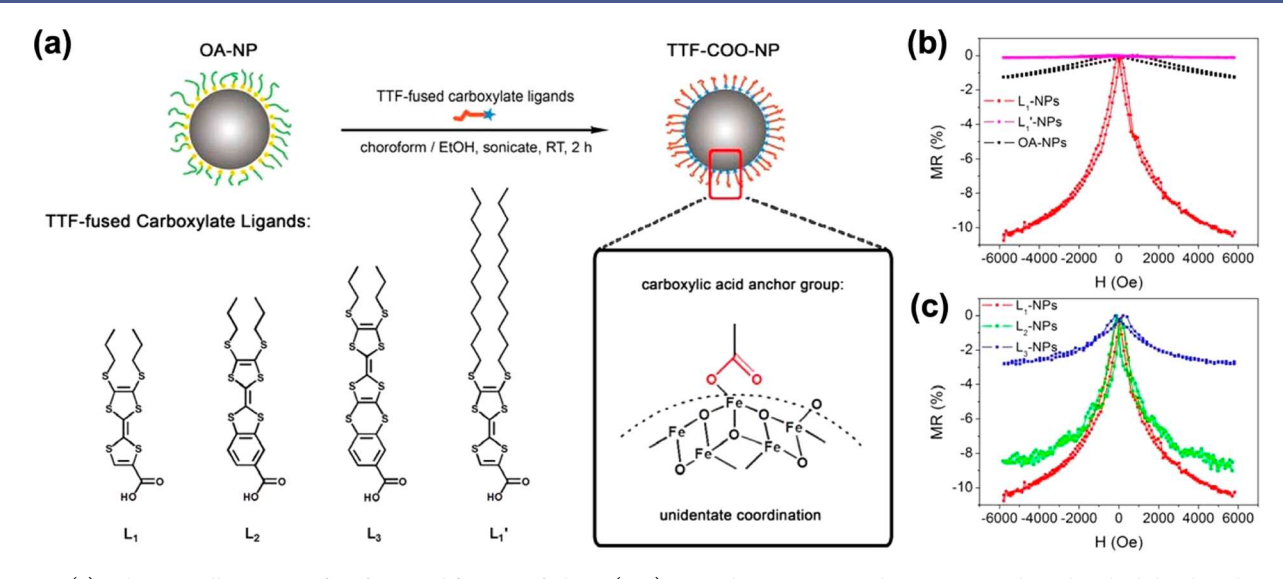


Figure 8. (a) Schematic illustration of surface modification of oleate (OA)-capped Fe_3O_4 NPs with TTF-COO⁻ ligands, which bind to the Fe_3O_4 surface via the monodentate Fe-O form. (b) Magnetic field MR of L_1 -, L_1 '-, and OA-NPs at 300 K. (c) Magnetic field MR of L_1 -, L_2 -, and L_3 -NPs at 100 K.⁴

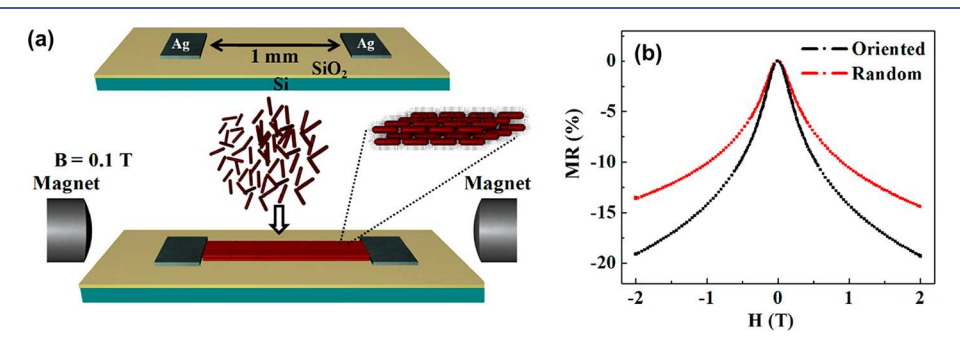


Figure 9. (a) Schematic illustration of deposition of oleylamine-coated Fe₃O₄ nanorods between two electrodes for studying TMR, and (b) MR curves of the oriented and randomly oriented nanorods show 19% and 14% MR, respectively.⁶⁴

to control both NP stability (against oxidation) and interparticle spacing (Figure 8a). Furthermore, the TTF-COO-Fe binding can also help to compensate the O-deficiency on the Fe₃O₄ NP surface, improving the spin polarization of the Fe₃O₄. After coating the TTF unit around 6 nm Fe₃O₄ NPs, their assemblies showed a 5% TMR ratio at room temperature. The NP array with shortest-chain ligand (L₁-NPs) has the largest MR ratio because it has the closest interparticle spacing in the NP assembly, which is controlled by the ligand chain length (Figure 6b,c). Besides the ligand length, the binding density of the TTF ligand can also be used to tune the MR ratio. A subsequent study investigated the impact of binding density of the TTF ligand by introducing an extra -COOH group on the basis of L₁.63 It showed that the extra O-chelate bonding led to a higher degree of the spin polarization on the Fe₃O₄ NP surface, thus higher TMR ratios in spin-dependent electron transport.

To further improve spin polarization and TMR properties, rod-shaped NPs are better adopted in the NP assembly due to the shape-induced magnetic anisotropy and higher interfacial area as compared to the spherical NPs. Recently, oleylamine-coated Fe₃O₄ nanorods were synthesized, assembled, and tested for TMR (Figure 9a). Magnetically aligned nanorods showed that the TMR was enhanced by a factor of 1.4 at room temperature as compared to randomly oriented nanorods (Figure 9b). The TMR value reached a maximum of 31% at

the Verwey transition temperature (120 K), and the spin polarization was calculated to be 46% at room temperature. This study also found that the shorter the nanorods, the smaller the TMR, suggesting that engineering NP anisotropic shape and ligand binding is a promising approach to tune the TMR behavior of ${\rm Fe_3O_4}$ nanostructures for broad spintronic applications.

5. CONCLUSION AND FUTURE OUTLOOK

Metal-ligand binding plays important roles in NP chemistry. Both binding mode and binding affinity can dictate NP formation, stabilization, and applications. The binding characteristics may be qualitatively explained by "hard and soft (Lewis) acids and bases" theory, and ligands selected for NP chemistry must facilitate NP growth, stabilization, and post-synthetic modification. The ligand chain should also be chemically stable in the NP synthetic process so that the metalligand roles in NP chemistry can be better understood. In this Account, we summarize the binding modes of some representative ligands that have been used extensively for synthesis and stabilization of monodisperse NPs. In general, a covalent bond is stronger than a coordination or an electrostatic one, and the metal-ligand binding can also be tailored to accommodate the next step reaction by tuning the solution pH and number of binding sites. We highlight some representative examples to show how to use metal-ligand

interactions to control NP sizes, compositions, and shapes in the synthetic reactions. The in situ X-ray studies and theoretical calculations further provide an obvious correlation between thermodynamics of metal-ligand binding and NP nucleation/growth rates. The composition of alloy NPs can be controlled by adjusting ratios of different ligands based on their preferential binding to the metals. Such metal-ligand binding chemistry is also extended to control anisotropic growth of NPs via selective ligand binding onto certain facets of NP surface or via seed-mediated growth of NPs in the anisotropic reverse micelles that are pre-formed by ligand molecule assembly in the synthetic solution. The ligand binding effects on NP functions have become a hot topic recently. We focus on ligand binding controlled electrochemical reduction of CO₂ with much improved activity, selectivity, and stability. As ligand length can be rationally tuned prior to its binding to NPs, interparticle spacing and electron transport across NP network can be more rationally regulated to show optimum performance. In all, the metal-ligand binding has played critical roles in NP synthesis, assembly, and property control.

The promising data presented in metal-ligand binding and their effects on NP chemistry call for in-depth understanding of metal-ligand binding thermodynamics and kinetics at NPligand interfaces and how these bindings affect properties of single NPs and ensembles of NPs. This requires not only precision synthesis but also timely advances of analytical and computational tools to guide the ligand selection and its molecular-level interactions at nanoscale interfaces. Precise engineering of NP-ligand interactions is essential to control NP formation, stability, and properties, which could have a huge impact on real-world applications. Recent studies have shown that ligand binding to NP surface provides a unique interfacial structure to control mass transport and electron tunneling across NPs. In electrocatalytic reduction of CO2, this represents a particularly promising direction for tuning the reduction selectivity toward a specific carbon product, and, in nanoelectronics, this provides an atomic level approach to functional devices that will be critical for spintronics and many other nanotechnological applications.

AUTHOR INFORMATION

Corresponding Author

Shouheng Sun — Department of Chemistry, Brown University, Providence, Rhode Island 02912, United States; orcid.org/0000-0002-4051-0430; Email: ssun@brown.edu

Authors

Huanqin Guan — Department of Chemistry, Brown University, Providence, Rhode Island 02912, United States;
orcid.org/0000-0002-8709-5262

Cooro Harris – Department of Chemistry, Brown University, Providence, Rhode Island 02912, United States

Complete contact information is available at: https://pubs.acs.org/10.1021/acs.accounts.3c00156

Notes

The authors declare no competing financial interest.

Biographies

Huanqin Guan obtained his B.S. degree from Peking University in 2018. He then came to the US and joined Prof. Shouheng Sun's group

and is currently a Ph.D. candidate in the Chemistry Department at Brown University. His research interests involve nanocatalyst synthesis and their applications in green chemistry reactions and ${\rm CO_2}$ capture and conversion.

Cooro Harris is a Ph.D. candidate in the Department of Chemistry at Brown University under Prof. Shouheng Sun as of 2023. They received their B.S. in chemistry with a minor in Japanese language and culture from Haverford College in 2019 before moving on to receive their M.A. in chemistry at Brown University. Their interests in the Sun Lab have focused on the application of heterogeneous nanocatalysts for accessing value-added products like polymers and CO₂ reduction products under mild and green conditions.

Shouheng Sun received his Ph.D. in Chemistry from Brown University in 1996. He joined the IBM T. J. Watson Research Center (Yorktown Heights, New York) first as a postdoctoral fellow (1996–1998) and then as a research staff member (1998–2004). In 2005, he returned to Brown University as a tenured Associate Professor and was promoted to full Professor in 2007. He is now the Vernon K. Krieble Professor of Chemistry and Professor of Engineering. His main research interests are in chemical synthesis and self-assembly of nanoparticles for catalytic, magnetic, and biomedical applications.

ACKNOWLEDGMENTS

This work was supported in part by the NSF under Grant CHE-2102290 and by Brown's Office of Vice President for Research.

REFERENCES

- (1) Shen, M.; Yu, C.; Guan, H.; Dong, X.; Harris, C.; Xiao, Z.; Yin, Z.; Muzzio, M.; Lin, H.; Robinson, J. R.; Colvin, V. L.; Sun, S. Nanoparticle-Catalyzed Green Chemistry Synthesis of Polybenzoxazole. *J. Am. Chem. Soc.* **2021**, *143*, 2115–2122.
- (2) Guan, H.; Shen, M.; Harris, C.; Lin, H.; Wei, K.; Morales, M.; Bronowich, N.; Sun, S. Cu₂O nanoparticle-catalyzed tandem reactions for the synthesis of robust polybenzoxazole. *Nanoscale* **2022**, *14*, 6162–6170.
- (3) Fu, J.; Zhu, W.; Chen, Y.; Yin, Z.; Li, Y.; Liu, J.; Zhang, H.; Zhu, J.-J.; Sun, S. Bipyridine-Assisted Assembly of Au Nanoparticles on Cu Nanowires To Enhance the Electrochemical Reduction of CO₂. *Angew. Chem., Int. Ed.* **2019**, *58*, 14100–14103.
- (4) Lv, Z.-P.; Luan, Z.-Z.; Wang, H.-Y.; Liu, S.; Li, C.-H.; Wu, D.; Zuo, J.-L.; Sun, S. Tuning Electron-Conduction and Spin Transport in Magnetic Iron Oxide Nanoparticle Assemblies via Tetrathiafulvalene-Fused Ligands. *ACS Nano* **2015**, *9*, 12205–12213.
- (5) Boles, M. A.; Ling, D.; Hyeon, T.; Talapin, D. V. The surface science of nanocrystals. *Nat. Mater.* **2016**, *15*, 141–153.
- (6) Yang, T.-H.; Shi, Y.; Janssen, A.; Xia, Y. Surface Capping Agents and Their Roles in Shape-Controlled Synthesis of Colloidal Metal Nanocrystals. *Angew. Chem., Int. Ed.* **2020**, *59*, 15378–15401.
- (7) Muzzio, M.; Li, J.; Yin, Z.; Delahunty, I. M.; Xie, J.; Sun, S. Monodisperse nanoparticles for catalysis and nanomedicine. *Nanoscale* **2019**, *11*, 18946–18967.
- (8) Ma, Z.; Mohapatra, J.; Wei, K.; Liu, J. P.; Sun, S. Magnetic Nanoparticles: Synthesis, Anisotropy, and Applications. *Chem. Rev.* **2023**, *123*, 3904.
- (9) Dreaden, E. C.; Alkilany, A. M.; Huang, X.; Murphy, C. J.; El-Sayed, M. A. The golden age: gold nanoparticles for biomedicine. *Chem. Soc. Rev.* **2012**, *41*, 2740–2779.
- (10) Lal, S.; Link, S.; Halas, N. J. Nano-optics from sensing to waveguiding. *Nat. Photonics* **2007**, *1*, 641–648.
- (11) Pietryga, J. M.; Park, Y.-S.; Lim, J.; Fidler, A. F.; Bae, W. K.; Brovelli, S.; Klimov, V. I. Spectroscopic and Device Aspects of Nanocrystal Quantum Dots. *Chem. Rev.* **2016**, *116*, 10513–10622.

- (12) Murray, C. B.; Sun, S.; Doyle, H.; Betley, T. Monodisperse 3d Transition-Metal (Co, Ni, Fe) Nanoparticles and Their Assembly into Nanoparticle Superlattices. *MRS Bull.* **2001**, *26*, 985–991.
- (13) Yin, Y.; Alivisatos, A. P. Colloidal nanocrystal synthesis and the organic—inorganic interface. *Nature* **2005**, *437*, 664–670.
- (14) Boles, M. A.; Engel, M.; Talapin, D. V. Self-Assembly of Colloidal Nanocrystals: From Intricate Structures to Functional Materials. *Chem. Rev.* **2016**, *116*, 11220–11289.
- (15) Lee, H.; Yoon, D.-E.; Koh, S.; Kang, M. S.; Lim, J.; Lee, D. C. Ligands as a universal molecular toolkit in synthesis and assembly of semiconductor nanocrystals. *Chem. Sci.* **2020**, *11*, 2318–2329.
- (16) Heuer-Jungemann, A.; Feliu, N.; Bakaimi, I.; Hamaly, M.; Alkilany, A.; Chakraborty, I.; Masood, A.; Casula, M. F.; Kostopoulou, A.; Oh, E.; Susumu, K.; Stewart, M. H.; Medintz, I. L.; Stratakis, E.; Parak, W. J.; Kanaras, A. G. The Role of Ligands in the Chemical Synthesis and Applications of Inorganic Nanoparticles. *Chem. Rev.* **2019**, *119*, 4819–4880.
- (17) De Nolf, K.; Capek, R. K.; Abe, S.; Sluydts, M.; Jang, Y.; Martins, J. C.; Cottenier, S.; Lifshitz, E.; Hens, Z. Controlling the Size of Hot Injection Made Nanocrystals by Manipulating the Diffusion Coefficient of the Solute. *J. Am. Chem. Soc.* **2015**, *137*, 2495–2505.
- (18) Howes, P. D.; Chandrawati, R.; Stevens, M. M. Colloidal nanoparticles as advanced biological sensors. *Science* **2014**, *346*, 1247390.
- (19) Goddard, Z. R.; Marín, M. J.; Russell, D. A.; Searcey, M. Active targeting of gold nanoparticles as cancer therapeutics. *Chem. Soc. Rev.* **2020**, *49*, 8774–8789.
- (20) Fan, J.; Cheng, Y.; Sun, M. Functionalized Gold Nanoparticles: Synthesis, Properties and Biomedical Applications. *Chem. Rec.* **2020**, 20, 1474–1504.
- (21) Shi, L.; Zhang, J.; Zhao, M.; Tang, S.; Cheng, X.; Zhang, W.; Li, W.; Liu, X.; Peng, H.; Wang, Q. Effects of polyethylene glycol on the surface of nanoparticles for targeted drug delivery. *Nanoscale* **2021**, 13, 10748–10764.
- (22) Zhang, W.; Mehta, A.; Tong, Z.; Esser, L.; Voelcker, N. H. Development of Polymeric Nanoparticles for Blood-Brain Barrier Transfer—Strategies and Challenges. *Adv. Sci.* **2021**, *8*, 2003937.
- (23) Cushing, B. L.; Kolesnichenko, V. L.; O'Connor, C. J. Recent Advances in the Liquid-Phase Syntheses of Inorganic Nanoparticles. *Chem. Rev.* **2004**, *104*, 3893–3946.
- (24) Wang, Y.; Counihan, M. J.; Lin, J. W.; Rodríguez-López, J.; Yang, H.; Lu, Y. Quantitative Analysis of DNA-Mediated Formation of Metal Nanocrystals. *J. Am. Chem. Soc.* **2020**, *142*, 20368–20379.
- (25) Wang, Y.; Satyavolu, N. s. R.; Yang, H.; Lu, Y. Kinetic Reconstruction of DNA-Programed Plasmonic Metal Nanostructures with Predictable Shapes and Optical Properties. *J. Am. Chem. Soc.* **2022**, *144*, 4410–4421.
- (26) Yao, Q.; Wu, Z.; Liu, Z.; Lin, Y.; Yuan, X.; Xie, J. Molecular reactivity of thiolate-protected noble metal nanoclusters: synthesis, self-assembly, and applications. *Chem. Sci.* **2021**, *12*, 99–127.
- (27) De Trizio, L.; Manna, L. Forging Colloidal Nanostructures via Cation Exchange Reactions. *Chem. Rev.* **2016**, *116*, 10852–10887.
- (28) Lee, S.; Yoon, D.-E.; Kim, D.; Shin, D. J.; Jeong, B. G.; Lee, D.; Lim, J.; Bae, W. K.; Lim, H.-K.; Lee, D. C. Direct cation exchange of CdSe nanocrystals into ZnSe enabled by controlled binding between guest cations and organic ligands. *Nanoscale* **2019**, *11*, 15072–15082.
- (29) Koh, S.; Kim, W. D.; Bae, W. K.; Lee, Y. K.; Lee, D. C. Controlling Ion-Exchange Balance and Morphology in Cation Exchange from Cu_{3-x}P Nanoplatelets into InP Crystals. *Chem. Mater.* **2019**, *31*, 1990–2001.
- (30) Lee, Y.; Loew, A.; Sun, S. Surface- and Structure-Dependent Catalytic Activity of Au Nanoparticles for Oxygen Reduction Reaction. *Chem. Mater.* **2010**, 22, 755–761.
- (31) Peng, S.; Lee, Y.; Wang, C.; Yin, H.; Dai, S.; Sun, S. A facile synthesis of monodisperse Au nanoparticles and their catalysis of CO oxidation. *Nano Res.* **2008**, *1*, 229–234.
- (32) Zhu, W.; Zhang, Y.-J.; Zhang, H.; Lv, H.; Li, Q.; Michalsky, R.; Peterson, A. A.; Sun, S. Active and Selective Conversion of CO₂ to

- CO on Ultrathin Au Nanowires. J. Am. Chem. Soc. 2014, 136, 16132–16135.
- (33) Wand, P.; Bartl, J. D.; Heiz, U.; Tschurl, M.; Cokoja, M. Functionalization of small platinum nanoparticles with amines and phosphines: Ligand binding modes and particle stability. *J. Colloid Interface Sci.* **2016**, 478, 72–80.
- (34) Li, W.; Taylor, M. G.; Bayerl, D.; Mozaffari, S.; Dixit, M.; Ivanov, S.; Seifert, S.; Lee, B.; Shanaiah, N.; Lu, Y.; Kovarik, L.; Mpourmpakis, G.; Karim, A. M. Solvent manipulation of the prereduction metal—ligand complex and particle-ligand binding for controlled synthesis of Pd nanoparticles. *Nanoscale* **2021**, *13*, 206—217.
- (35) Mantella, V.; Strach, M.; Frank, K.; Pankhurst, J. R.; Stoian, D.; Gadiyar, C.; Nickel, B.; Buonsanti, R. Polymer Lamellae as Reaction Intermediates in the Formation of Copper Nanospheres as Evidenced by In Situ X-ray Studies. *Angew. Chem., Int. Ed.* **2020**, *59*, 11627–11633
- (36) Yu, Y.; Yang, W.; Sun, X.; Zhu, W.; Li, X. Z.; Sellmyer, D. J.; Sun, S. Monodisperse MPt (M = Fe, Co, Ni, Cu, Zn) Nanoparticles Prepared from a Facile Oleylamine Reduction of Metal Salts. *Nano Lett.* **2014**, *14*, 2778–2782.
- (37) Liu, Y.; Chi, M. F.; Mazumder, V.; More, K. L.; Soled, S.; Henao, J. D.; Sun, S. Composition-Controlled Synthesis of Bimetallic PdPt Nanoparticles and Their Electro-oxidation of Methanol. *Chem. Mater.* **2011**, 23, 4199–4203.
- (38) Sun, S. Recent Advances in Chemical Synthesis, Self-Assembly, and Applications of FePt Nanoparticles. *Adv. Mater.* **2006**, *18*, 393–403
- (39) Sun, S.; Murray, C. B.; Weller, D.; Folks, L.; Moser, A. Monodisperse FePt Nanoparticles and Ferromagnetic FePt Nanocrystal Superlattices. *Science* **2000**, 287, 1989–1992.
- (40) Wu, L.; Mendoza-Garcia, A.; Li, Q.; Sun, S. Organic Phase Syntheses of Magnetic Nanoparticles and Their Applications. *Chem. Rev.* **2016**, *116*, 10473–10512.
- (41) Bhattacharjee, K.; Prasad, B. L. V. Surface functionalization of inorganic nanoparticles with ligands: a necessary step for their utility. *Chem. Soc. Rev.* **2023**, *52*, 2573–2595.
- (42) Jun, Y.-w.; Choi, J.-s.; Cheon, J. Shape Control of Semiconductor and Metal Oxide Nanocrystals through Nonhydrolytic Colloidal Routes. *Angew. Chem., Int. Ed.* **2006**, *45*, 3414–3439.
- (43) Zheng, J.; Cheng, X.; Zhang, H.; Bai, X.; Ai, R.; Shao, L.; Wang, J. Gold Nanorods: The Most Versatile Plasmonic Nanoparticles. *Chem. Rev.* **2021**, *121*, 13342–13453.
- (44) Janicek, B. E.; Hinman, J. G.; Hinman, J. J.; Bae, S. h.; Wu, M.; Turner, J.; Chang, H.-H.; Park, E.; Lawless, R.; Suslick, K. S.; Murphy, C. J.; Huang, P. Y. Quantitative Imaging of Organic Ligand Density on Anisotropic Inorganic Nanocrystals. *Nano Lett.* **2019**, *19*, 6308–6314
- (45) Wang, C.; Hou, Y.; Kim, J.; Sun, S. A General Strategy for Synthesizing FePt Nanowires and Nanorods. *Angew. Chem., Int. Ed.* **2007**, *46*, 6333–6335.
- (46) Peng, Z.; You, H.; Yang, H. Composition-Dependent Formation of Platinum Silver Nanowires. *ACS Nano* **2010**, *4*, 1501–1510.
- (47) Wei, K.; Guan, H.; Luo, Q.; He, J.; Sun, S. Recent advances in CO₂ capture and reduction. *Nanoscale* **2022**, *14*, 11869–11891.
- (48) Niu, Z.; Li, Y. Removal and Utilization of Capping Agents in Nanocatalysis. *Chem. Mater.* **2014**, *26*, 72–83.
- (49) Xie, C.; Niu, Z.; Kim, D.; Li, M.; Yang, P. Surface and Interface Control in Nanoparticle Catalysis. *Chem. Rev.* **2020**, *120*, 1184–1249. (50) Lu, L.; Zou, S.; Fang, B. The Critical Impacts of Ligands on Heterogeneous Nanocatalysis: A Review. *ACS Catal.* **2021**, *11*, 6020–6058.
- (51) Tamura, J.; Ono, A.; Sugano, Y.; Huang, C.; Nishizawa, H.; Mikoshiba, S. Electrochemical reduction of CO_2 to ethylene glycol on imidazolium ion-terminated self-assembly monolayer-modified Au electrodes in an aqueous solution. *Phys. Chem. Chem. Phys.* **2015**, *17*, 26072–26078.

Accounts of Chemical Research

- (52) Zhang, L.; Wei, Z.; Thanneeru, S.; Meng, M.; Kruzyk, M.; Ung, G.; Liu, B.; He, J. A Polymer Solution To Prevent Nanoclustering and Improve the Selectivity of Metal Nanoparticles for Electrocatalytic CO₂ Reduction. *Angew. Chem., Int. Ed.* **2019**, *58*, 15834–15840.
- (53) Shen, H.; Tian, G.; Xu, Z.; Wang, L.; Wu, Q.; Zhang, Y.; Teo, B. K.; Zheng, N. N-heterocyclic carbene coordinated metal nanoparticles and nanoclusters. *Coord. Chem. Rev.* **2022**, 458, 214425.
- (54) Hopkinson, M. N.; Richter, C.; Schedler, M.; Glorius, F. An overview of N-heterocyclic carbenes. *Nature* **2014**, *510*, 485–496.
- (55) Engel, S.; Fritz, E.-C.; Ravoo, B. J. New trends in the functionalization of metallic gold: from organosulfur ligands to N-heterocyclic carbenes. *Chem. Soc. Rev.* **2017**, *46*, 2057–2075.
- (56) Akter, T.; Pan, H.; Barile, C. J. Tandem Electrocatalytic CO₂ Reduction inside a Membrane with Enhanced Selectivity for Ethylene. *J. Phys. Chem. C* **2022**, *126*, 10045–10052.
- (57) Kim, D.; Yu, S.; Zheng, F.; Roh, I.; Li, Y.; Louisia, S.; Qi, Z.; Somorjai, G. A.; Frei, H.; Wang, L.-W.; Yang, P. Selective CO₂ electrocatalysis at the pseudocapacitive nanoparticle/ordered-ligand interlayer. *Nat. Energy* **2020**, *5*, 1032–1042.
- (58) Coropceanu, İ.; Janke, E. M.; Portner, J.; Haubold, D.; Nguyen, T. D.; Das, A.; Tanner, C. P. N.; Utterback, J. K.; Teitelbaum, S. W.; Hudson, M. H.; Sarma, N. A.; Hinkle, A. M.; Tassone, C. J.; Eychmüller, A.; Limmer, D. T.; Olvera de la Cruz, M.; Ginsberg, N. S.; Talapin, D. V. Self-assembly of nanocrystals into strongly electronically coupled all-inorganic supercrystals. *Science* **2022**, 375, 1422–1426.
- (59) Li, D.; Chen, Q.; Chun, J.; Fichthorn, K.; De Yoreo, J.; Zheng, H. Nanoparticle Assembly and Oriented Attachment: Correlating Controlling Factors to the Resulting Structures. *Chem. Rev.* **2023**, *123*, 3127–3159.
- (60) Escudero, A.; González-García, L.; Strahl, R.; Kang, D. J.; Drzic, J.; Kraus, T. Large-Scale Synthesis of Hybrid Conductive Polymer—Gold Nanoparticles Using "Sacrificial" Weakly Binding Ligands for Printing Electronics. *Inorg. Chem.* **2021**, *60*, 17103–17113.
- (61) Zhou, B. H.; Rinehart, J. D. A Size Threshold for Enhanced Magnetoresistance in Colloidally Prepared CoFe₂O₄ Nanoparticle Solids. ACS Cent. Sci. 2018, 4, 1222–1227.
- (62) Coey, J. M. D.; Berkowitz, A. E.; Balcells, L.; Putris, F. F.; Parker, F. T. Magnetoresistance of magnetite. *Appl. Phys. Lett.* **1998**, 72, 734–736.
- (63) Lv, Z.-P.; Luan, Z.-Z.; Cai, P.-Y.; Wang, T.; Li, C.-H.; Wu, D.; Zuo, J.-L.; Sun, S. Enhancing magnetoresistance in tetrathiafulvalene carboxylate modified iron oxide nanoparticle assemblies. *Nanoscale* **2016**, *8*, 12128–12133.
- (64) Mitra, A.; Mohapatra, J.; Sharma, H.; Meena, S. S.; Aslam, M. Controlled synthesis and enhanced tunnelling magnetoresistance in oriented Fe₃O₄ nanorod assemblies. *J. Phys. D: Appl. Phys.* **2018**, *51*, 085002.